GSICS Global Space-based Inter-Calibration System

Quarterly Newsletter

Volume 7 Number 3
2013
Fall Issue

doi:10.7289/V5N877QQ

Manik Bali, Editor

CMA • CNES • EUMETSAT • IMD • ISRO • JAXA • JMA • KMA • NASA • NIST • NOAA • ROSHYDROMET • USGS • WMO

This Issue:

Lunar Calibration

In This Issue

Moon as a Calibration Source:

Physical Basis and Background

by Tom Stone, USGS

Interest in using the Moon for an on-orbit radiometric reference is driven by the unique calibration capabilities that are made possible by its inherent physical properties. The Moon is accessible to potentially all instruments in any Earth orbit, with no intervening atmosphere. Regarded as a calibration light source at reflected solar wavelengths, the Moon is effectively a solar diffuser whose surface reflectance is exceptionally stable; it is considered invariant to under one part in 10^8 per year (Kieffer, 1997). This allows radiometric measurements from lunar observations to be compared regardless of the time interval between the acquisitions.

Because the reflectance of the lunar surface is non-uniform and highly non-Lambertian, the lunar radiometric reference must take the form of an analytic model that can be computed for any particular set of conditions of an instrument's observations. Developing such a model requires an extensive set of characterization measurements to capture the periodic lunar brightness variations, primarily the changes with phase. The accuracy of the model specification is directly related to the extent of the basis measurement dataset, which can span several years. To utilize the Moon as an irradiance source adds the complication that the brightness also depends on the particular hemispheres of the Moon that are illuminated and viewed, known as the lunar librations. But using the irradiance quantity avoids the need for spatial co-registration of an instrument's observations with a spatially resolved (i.e. radiance) lunar reference, which can be a substantial task.

The concept of using the Moon for on-orbit radiometric calibration (Kieffer and Wildey, 1985) was developed from albedo studies of the lunar surface done in the 1960s in support of the Apollo spaceflight program. The Lunar Calibration facility and the Robotic Lunar Observatory (ROLO; Kieffer and Wildey, 1996) were established at the

USGS Astrogeology Science Center in Flagstaff, Arizona, under sponsorship from the NASA Earth Observing System (EOS) program. From 1995 to 2003, ROLO acquired images of the Moon and stars every clear night from First Quarter to Last Quarter lunar phases. These images form the basis dataset for the lunar spectral irradiance model (Kieffer and Stone, 2005) used by the USGS for lunar calibration services. This model accounts for the lunar brightness variations with geometry, i.e. the phase and librations, with high precision, and includes a specification of the small-angle backscatter enhancement known as the opposition effect.

Routine Moon observations by spacecraft instruments have been conducted for many years, and data processing groups have incorporated lunar calibration results into the generation of level-1 data products, notably for SeaWiFS, MODIS Terra and Aqua, and NPP-VIIRS. To date, the USGS lunar calibration system has been used mostly for relative calibrations, e.g. long-term stability monitoring and cross-calibration. It is not typically used for absolute calibration due to the lack of SI-traceability in the ROLO absolute radiometric scale, and the uncertainty of this scale is in the 5-10% range. But the current limitations of lunar calibration are due solely to the uncertainties in the models. The Moon itself can be characterized to the accuracy limits of field measurement technology, and it is feasible that the lunar reference can be specified, via models, to nearly these same levels of accuracy. This is a high priority in this area.

This issue of GSICS Quarterly examines some recent developments that have spurred advancement of lunar calibration capabilities. Substantial datasets of Moon observations have been acquired from geostationary orbit by the Meteosat SEVIRI instruments, and from low Earth orbit by the highly agile PLEIADES spacecraft operated by CNES. The unprecedented density and quality of these space-based measurements have revealed residual dependencies in the specification of lunar irradiance provided by the USGS model. A NIST-led measurement effort is addressing the need for a high-accuracy, SI-traceable absolute lunar irradiance reference. An application of lunar calibration to GOES visible-channel imagers provides an example of using the Moon to evaluate subtle instrument response effects.

References:

Kieffer, H.H., 1997, Photometric Stability of the Lunar Surface. *Icarus*, 130, 323-327.

Keiffer, H. H., and Stone, T.C., 2005, The Spectral Irradiance of the Moon, *Astron. J.*, 129, 2887-2901.

Rate and comment on this article

Absolute Calibration of Lunar Spectral Irradiance

by Claire Cramer, NIST

The utility of the Moon as an on-orbit radiometric calibration source at reflected solar wavelengths is limited by measurement uncertainty in the absolute scale of lunar spectral irradiance. While the USGS model mentioned allows the Moon to be used for relative calibrations with sub-percent accuracy, the model's lack of SI-traceability and relatively large uncertainty (thought to be 5-10%) prevent the Moon's use for absolute calibration. Establishing an accurate scale for lunar spectral irradiance traceable to the SI would therefore greatly enhance the value of the USGS model for on-orbit calibrations of remote sensing instruments.

The National Institute of Standards and Technology (NIST) has recently demonstrated that it is possible to calibrate the Moon's spectral irradiance with a standard combined uncertainty below 1% (k=1) at reflected solar wavelengths using a ground-based telescope calibrated nightly with laboratory standards adapted for use in the field. The NIST pilot study used a small telescope to direct moonlight into an integrating sphere, which homogenizes the incident light and ensures that the measurement is insensitive to polarization and pointing accuracy. The homogenized moonlight was transmitted to a stable laboratory spectrometer through a flexible optical light guide attached to a port on the integrating sphere. The telescope, integrating sphere, light guide, and spectrometer were calibrated as a unit several times throughout each night's lunar observations using a large, lamp-illuminated integrating sphere and NIST-calibrated spectrometer as transfer standards. SI-traceability is established through the NIST calibration of the second spectrometer, which was repeated before and after each observing run.

The pilot study was performed at an elevation of 2,367 m on the ridge of Mt. Hopkins in southern Arizona. Because this elevation is near the top of the boundary layer, the tropospheric aerosol optical depth at the observatory on a clear night is extremely low. It is, however, necessary to carefully account for stratospheric aerosols, ozone absorption, and the pressure and temperature dependence of Rayleigh scattering in the atmosphere. When the atmosphere is temporally stable and isotropic, it is possible to use the Beer-Lambert-Bougher law together with the USGS model and independent measurements of the total ozone column and local temperature and pressure profile to extract the lunar spectral irradiance at the top of the atmosphere from a time series of lunar spectra collected throughout the night. Figure 1 shows the calibrated lunar spectral irradiance on a night with near-ideal atmospheric conditions. No attempt was made to account for strong molecular absorption (from O_2 and H_2O) in the pilot study, though it is theoretically possible to do so. The measurement uncertainty, shown in the lower panel of Figure 1, is greater than 1% below 420 nm and above 1000 nm due to low signal in the spectrograph.

Between 420 nm and 1000 nm, the uncertainty is dominated by the NIST calibration establishing SI-traceability.

The NIST pilot study demonstrates that it should be possible to establish an absolute scale for the USGS model that allows on-orbit lunar calibration to be a viable solution for many remote sensing instruments. This could readily be accomplished by placing the lunar telescope apparatus at a well-characterized high altitude site such as the NOAA observatory on Mauna Loa for several years to provide good coverage of the phase-libration angle parameter space. The wavelength range could be extended into the short-wave infrared by adapting the apparatus for flight on a balloon or aircraft above tropospheric water vapor.

Reference:

Cramer, C.E., Lykke, K.R., Woodward, J.T., and Smith, A.W., 2013, Precise Measurement of Lunar Spectral Irradiance at Lunar Wavelengths, *J Res NIST*, 188, 396-402.

Rate and comment on this article

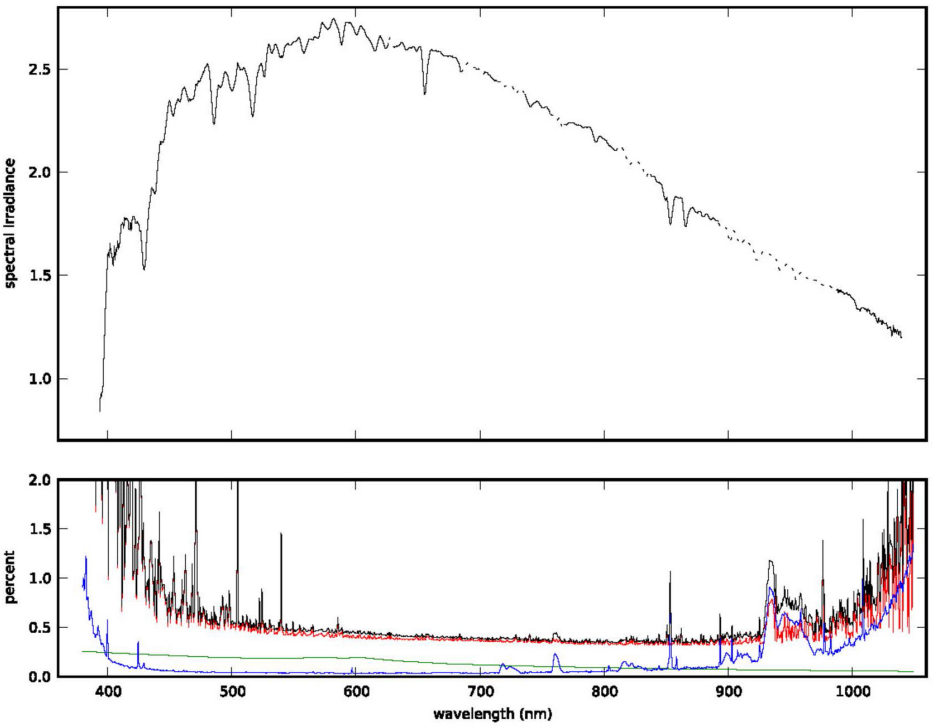

Figure 1: Spectral irradiance of the Moon in units of μW m^{-2} nm^{-1} at 11:40:43 on 30 November, 2012 UT (top panel) at (31 41 1.5 N, 110 52 40.8 W). The associated uncertainty in the linear fit (blue), combined uncertainty in the corrections for ozone and stratospheric aerosols (green), uncertainty in the calibration (red), and total combined uncertainty (black) are shown in the lower panel. The measurement is valid with the uncertainty shown here in the regions of the spectrum not affected by strong molecular absorption. At wavelengths where the discrepancy between our measured Rayleigh transmission and the expected Rayleigh transmission is greater than 1% , we scale the USGS model prediction to produce the dotted line in the upper panel.

Lunar Calibration of MSG/SEVIRI Solar Bands

by Bartolomeo Viticchié, EUMETSAT, Sébastien Wagner, EUMETSAT, Tim Hewison, EUMETSAT, and Tom Stone, USGS

The SEVIRI imagers aboard the Meteosat Second Generation (MSG) platforms produce images in twelve spectral bands in the wavelength range 0.56-14.4µm. SEVIRI has four solar bands, namely, the VIS06, the VIS08, the NIR16, and the High spatial Resolution VISible (HRVIS; Schmetz et al., 2002). For these bands absolute calibration accuracy 2% for long-term stability is required.

The calibration of the SEVIRI solar bands is based on a vicarious calibration technique using stable desert scenes as transfer targets (Govaerts et al., 2004). Such a method provides the calibration coefficients and allows one to monitor the sensor temporal drift. However, several years are required to derive reliable drift estimates and to reduce the uncertainties caused by seasonal variations and changes in surface properties of the targets.

To overcome these limitations the Moon can be employed as a complementary target for drift monitoring. In fact, this crosses regularly the SEVIRI field of regard and it can be used as a radiometric reference by means of the ROLO model (Kieffer & Stone, 2005).

In order to monitor the drift of the four SEVIRI solar bands using the Moon, a prototype of lunar calibration system has been implemented at EUMETSAT. This is composed of two parts:

- Archive of lunar observations,
- Calibration procedure based on the ROLO model (implemented and validated in collaboration with Tom Stone).

The data archive is currently composed by 542 low-res (Moon available in all bands) plus 70 HRVIS Moon observations from MSG1 (covering the time window 2003 – present); 420 low-res plus 91 HRVIS observations

Return to Page 1

from MSG2 (covering the time window 2006 – present). This dataset is a unique collection of Moon observations covering a wide range of both illumination and libration angles.

The output produced by the calibration procedure is the difference between the observed total Moon disk irradiance and the modeled ROLO irradiance expressed as:

$$\Delta Irr = 100 \bullet \left(1-\frac{Irr_{OBS}}{Irr_{ROLO}}\right) [\%].$$

Here we will not focus on the absolute value of this difference since the ROLO model is being used exclusively to monitor the temporal stability of SEVIRI. It is important to specify that the results that will be presented here have been corrected for the phase angle dependence shown in "*On the phase-angle dependence of the Moon calibration results*" also published in this issue**.**

The results obtained for MSG1 as a function of the Julian day are represented in Figure 1. The temporal stability of the bands is here described by the standard deviation (σ) with respect to the average difference over the complete dataset (< >). In Figure 1 σ ≤ 1.4% for all the bands. The time sequence for the VIS06 band presents a negative trend which is particularly evident starting from 2009. Another interesting feature is found in the NIR16 sequence between the beginning of 2005 and the end of 2008. During this period *ΔIrr* increases about 2% and remains constant over four years. At the beginning of 2009 the value of *ΔIrr* goes back to the initial value.

For MSG2 (Figure 2), three of the four bands (i.e., the VIS06, the VIS08, and the HRVIS) have a standard deviation with respect to the average difference between 1.1% and 1.5%. Moreover, in these three bands an important trend is found between the beginning of 2010 and 2013 which brings a reduction of *ΔIrr* of about 4% in three years. The NIR16 band is very stable with a standard deviation with respect to the average of 0.91% and no significant trend.

These results show that both MSG1 and MSG2 satisfy the long term stability requirements specified above. In spite of

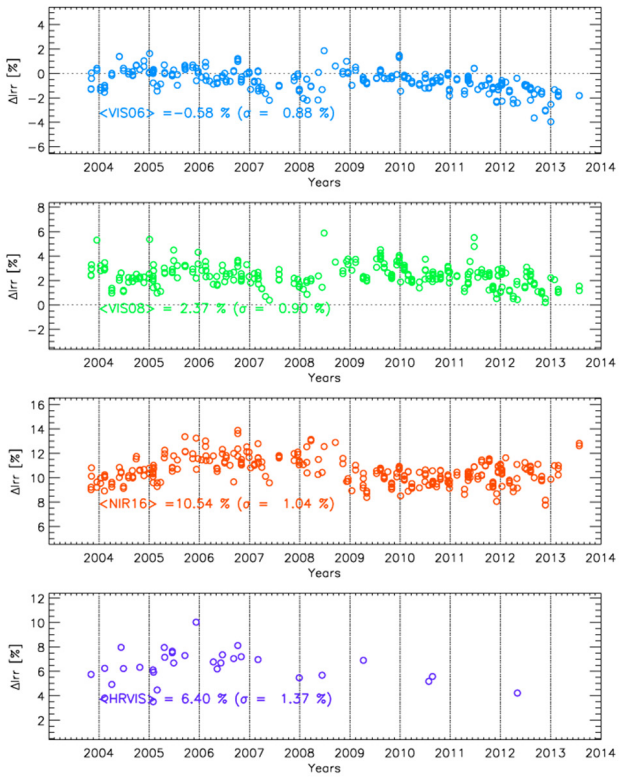

Figure 1: Results of the lunar calibration applied to the MSG1 dataset. The outputs are represented as a function of the Julian day in four different panels, one panel per band (from the top, VIS06, VIS08, NIR16, and HRVIS). In each panel: i) the circles represent the output of the ROLO calibration; ii) average value of Δ*Irr* (< >) over the complete dataset together with the standard deviation with respect to the mean (σ).

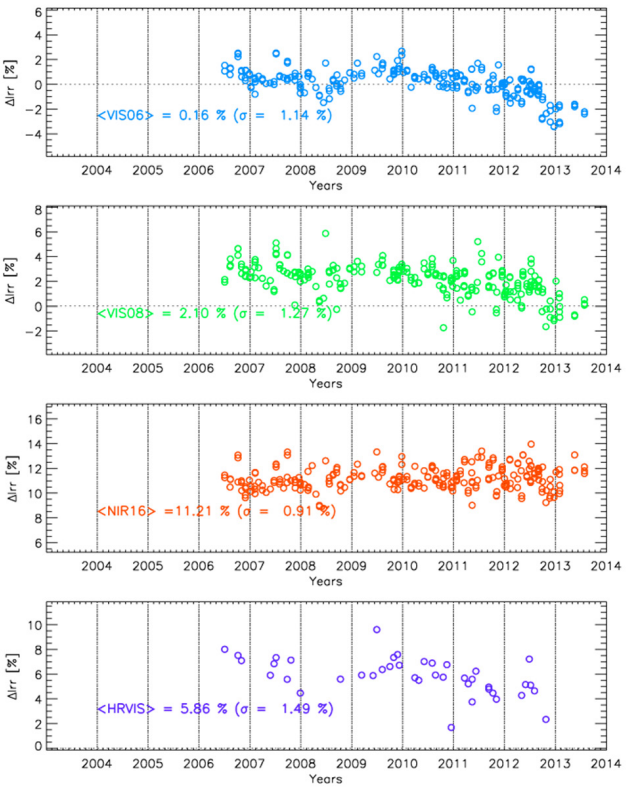

Figure 2: Mosaic plot of the results of the calibration procedure applied to the MSG2 dataset. Same format of Figure 1.

Return to Page 1

this, the trends and the features found in the time sequences of both Figure 1 and Figure 2 deserve a more detailed study in order to be fully understood.

Finally, after the tests performed in collaboration with Tom Stone, the lunar calibration procedure implemented at EUMETSAT can be considered reliable and will be applied on a regular base in the next years also on MSG3 data.

References:

Govaerts, Y. M., Clerici, M., and Clerbaux, N., 2004, *IEEE Transactions on Geoscience and Remote Sensing*, 42, 1900

Kieffer, H., H., and Stone, T. C., 2005, *The Astronomical Journal*, 129, 2887.

Schmetz, J., Pili, P., Tjemkes, S., et al., 2002, *Bulletin of the American Meteorological Society*, 83, 977.

Rate and comment on this article

Pleiades Orbital Lunar Observations (POLO) - Intensive Study of the Moon

by Sophie Lachérade, CNES

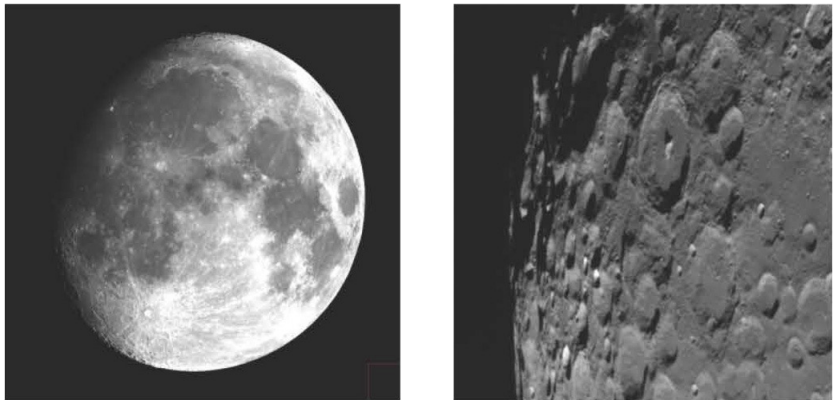

Figure 1: The Moon as seen by PHR-1A. One Moon image consists of more than 4 million pixels. The figure on the right illustrates the Moon in full resolution.

The PHR (PLEIADES High Resolution) program is a space Earth Observation system operated by France, under the leadership of CNES. It operates in 2013 two agile satellites, PHR-1A and PHR-1B, launched in 2011 and 2012, respectively, designed to provide optical images to civilian and defence users. Images are simultaneously acquired in Panchromatic and multi-spectral mode, which allows, in nadir acquisition condition, to deliver 20km wide, false or natural colored scenes with a 70cm ground sampling distance in panchromatic mode and 2.8m for the multispectral bands.

One of the major improvements of this satellite is its platform agility. It allows the satellite to move quickly from one attitude to another, enabling rapid collection of separated point targets and an increase of imaging capacity. It also allows acquisitions of extraterrestrial objects such as stars and the Moon.

This article focuses on the activities conducted during the commissioning phase of PHR-1A and PHR-1B aimed at the absolute radiometric calibration of the sensors and especially on the analysis of the Moon acquisitions.

The moon is one of the natural sites used for the PHR radiometric calibration. In a nominal calibration mode, the moon is observed once a month during the descending phase (40°±1° phase angle) in order to follow the stability of the sensor's different spectral bands. The lunar calibration method is based on the model USGS RObotic Lunar Observatory (ROLO), developed by (Kieffer and Stone, 2005). This semi-empirical model takes into account both the phase angle and the lunar librations of the Moon and is able to simulate the global reflectance of the Moon at any date. For each lunar acquisition, the calibration method consists in calculating a standardized lunar irradiance I_{obs}, integrated over the spectral range of the sensor:

$$I_{obs} = \frac{\sum_{i=1}^{N_p} L_i \cdot \Omega_i}{A_l(\alpha_l)} \cdot \left(\frac{D_{l-obs}}{384400}\right)^2 \left(\frac{D_{l-s}}{1AU}\right)^2$$

where L is the radiance measured by each pixel of the sensor within the solid angle Ω and A is the equivalent ROLO albedo integrated over the spectral bands of PLEIADES. This value is in theory invariant and only depends on the sensitivity of the instrument.

Taking advantage of the high level of agility of PHR, we performed an intensive observation campaign of the Moon in addition to the nominal acquisitions – when the Moon phase angle is about 40°. This intensive study of the Moon consists of several hundred acquisitions, which were acquired during the commissioning phases of the two PHR satellites. The Moon was acquired as frequently as one every orbit, which represents acquisitions every 100 minutes, for several phase cycles covering the phase angle range ±115 deg (Figure 2).

The goal of this study was to better understand the sensitivity of our new calibration method and to be able to answer the following questions:

What is the impact of the dark signal (background noise) on the integrated signal of the moon?

How to integrate it precisely?

What is the impact of the geometrical sampling of the sensor on the calibration results?

What is the sensitivity of the method to the moon phase angle, including in the extrapolation part of the ROLO model (over 90°)?

What is the sensitivity of the method regarding the position of the sensor on its orbit?

Answering these questions will provide valuable inputs and recommendations for a better use of lunar acquisitions.

References

Kieffer, H., H., and Stone, T. C., 2005, The spectral irradiance of the Moon. *The Astronomical Journal*, 129, 2887-2901.

Lachérade, S., Fourest S., Gamet P., Lebègue L., 2012, PLEIADES absolute calibration: inflight calibration sites and methodology, *XXII[nd] ISPRS Conference*, Melbourne, Australia

Rate and comment on this article

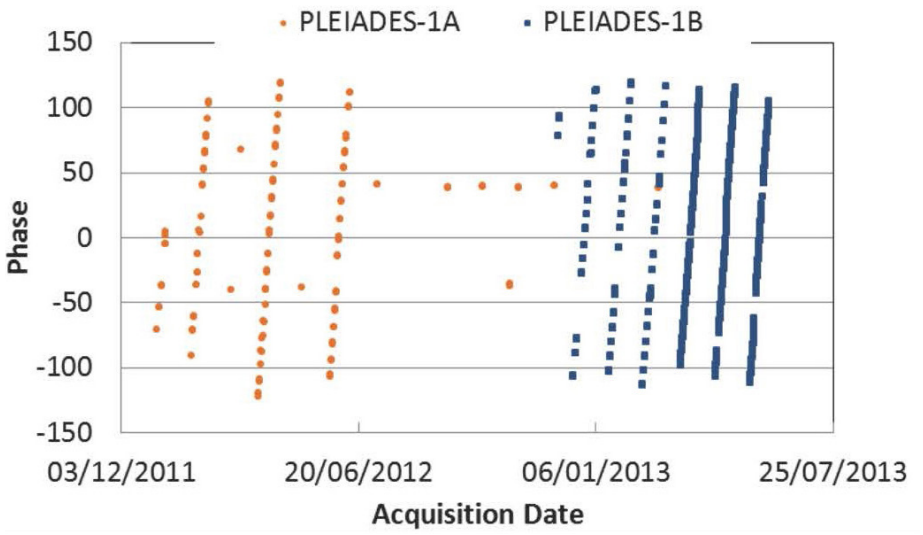

Figure 2: Temporal distribution of the lunar acquisitions of PHR-1A (red dots) and PHR-1B (blue square) during the commissioning phases.

On the Phase-Angle Dependence of the Moon Calibration Results

by Sophie Lachérade, CNES, Bartolomeo Viticchié, EUMETSAT, Tom Stone, USGS, Laurent Lebègue, CNES, Sebastien Wagner, EUMETSAT, and Tim Hewison, EUMETSAT

Using the Moon as a calibration target requires knowing how its brightness (reflectance) changes with: phase angle, lunar librations, non-uniform surface albedo, and non-Lambertian reflectance. By mastering all the phenomena affecting the Moon brightness one can estimate the Moon irradiance at any time (including in the past).

A unique tool for modeling the lunar irradiance (reflectance) is the Robotic Lunar Observation (ROLO) model of Kieffer & Stone (2005).

In the following we will focus on the phase angle dependence of the ROLO calibration by analyzing two unique datasets from Earth-orbiting satellites which cover a wide range of phase angle. These are:

1. The archive of lunar observations extracted from the solar channels of MSG/SEVIRIs available at EUMETSAT.
2. Dedicated lunar images obtained with PLEIADES-1A and PLEIADES-1B available at CNES.

The SEVIRI imagers aboard the Meteosat Second Generation (MSG) platforms observe the Earth from Geostationary orbits in twelve spectral bands between 0.56µm and 14.4µm. Four of these bands are solar bands, namely, the VIS06, the VIS08, the NIR16, and the High spatial Resolution VISible (HRVIS). These are the bands of SEVIRI, which can be calibrated using the ROLO model. 542 observations of the Moon, acquired simultaneously in the VIS06, VIS08, and NIR16 (low-res) plus 70 observations in the HRVIS have been extracted from MSG1 (spanning the years 2003 – present), and 430 low-res plus 91 HRVIS observations from MSG2 (spanning the years 2006 – present). The phase angle range covered by this datasets is ±120 deg. Moreover, the distribution of the phase angle samples is rather uniform within the range. Another important characteristic of this dataset is that it covers a wide range of libration angles (due to its temporal extension).

The second dataset corresponds to very high spatial resolution images of the Moon acquired by the two satellites PLEIADES-1A and PLEIADES-1B respectively launched at the end of 2011 and 2012. This imagery system, operated by CNES, is composed of four spectral bands: BLUE, GREEN, RED

Return to Page 1

and NIR, with a resolution of 2.8m in vertical earthward viewing and one panchromatic band with a resolution of 0.7 m in vertical earthward viewing. The commissioning phases of these satellites were a unique occasion to perform an intensive observation campaign of the Moon dedicated to evaluating the sensitivity of calibration methods using the Moon. For this purpose, CNES performed Moon acquisitions as frequently as one every orbit, which represents one acquisition every 100 minutes, for several phase cycles covering the phase angle range ±115 deg. After six months, more than 800 images of the Moon were acquired covering a wide range of phase conditions. One of the most important advantages of this intensive study is that the images of the Moon are not affected by the PLEIADES calibration, which has been proven to remain very stable during this short period of time.

The two datasets were analyzed by exploiting two independent calibration procedures both based on the ROLO model of Kieffer & Stone (2005). The procedures were validated in collaboration with Tom Stone and successfully cross-checked for consistency.

In Figure 1, we show the differences between the modeled ROLO irradiance and the Moon irradiance observed by MSG2 SEVIRI/VIS06 and PLEIADES-1B/B2: $\Delta Irr = 100 \cdot \left(1-\frac{Irr_{OBS}}{Irr_{ROLO}}\right)$ [%], as a function of the signed phase angle. Both bands correspond to the red region of the spectrum. These have been shifted vertically one over the other to ease the comparison of the results.

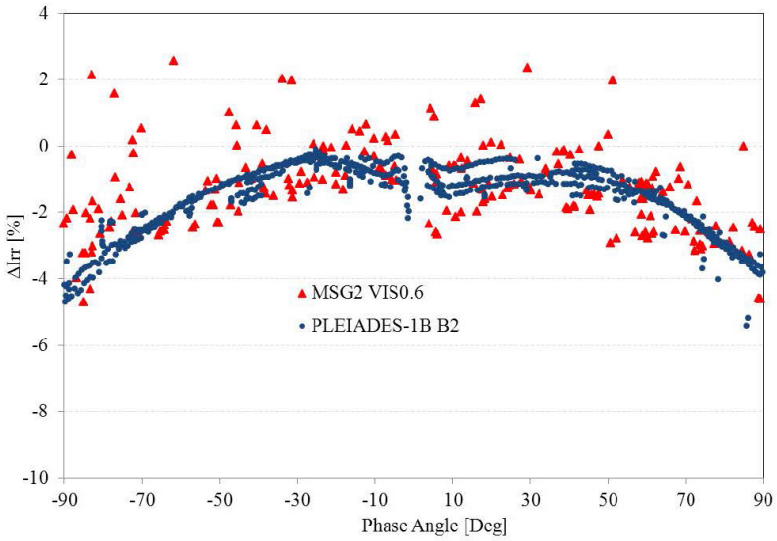

Figure 1: Comparison of the calibration result ΔIrr as a function of the phase angle obtained from the dataset of MSG2 (SEVIRI/VIS06, red triangles) and PLEIADES 1B (B2, blue dots).

SEVIRI and PLEIADES show a good agreement in the shape of this phase angle dependence which reaches about 4% at ±90 deg phase angle (Figure 1). This dependence was already highlighted by Eplee et al. (2011) on the SeaWiFS dataset for large phase angles up to ±90 deg.

Due to the high precision of the lunar irradiance measurements made from the PLEIADES data, we are able to see on the results a small asymmetry with respect to 0. This might stem from the fact that in the PLEIADES dataset the lunar brightness changes with the phase angle exclusively (the dataset has been acquired in a very short time so that the libration angle can be considered constant). This is not the case for the SEVIRI's dataset in which the libration angle varies significantly together with the phase angle. Moreover, the spatial resolution of PLEIADES might play a key role in revealing the differences between the two halves of the lunar disk illuminated for positive and negative phase angles. More work is needed to fully understand these results.

This phase angle dependence could strongly affect instruments which cannot choose the Moon phase for their calibration. For this reason, an improvement of the ROLO model, based on the PLEIADES data, could be planned in the near future.

References:

Eplee, R. E., Jr., Sun, J., Meister, G., et al., 2011, *Applied Optics*, 50, 120.

Kieffer, H., H., and Stone, T. C., 2005, *The Astronomical Journal*, 129, 2887.

[Rate and comment on this article]

Calibration/Validation of Suomi-NPP/VIIRS Day-Night Band using Moon Light

by Dr. Xi Shao, Dr. Changyong Cao, and Sirish Uprety *from NOAA/NESDIS/STAR*

The Day Night Band (DNB) of the Visible Infrared Imaging Radiometer Suite (VIIRS) onboard Suomi-NPP (Cao et al., 2013) represents a major advancement in night time imaging capabilities. The DNB of the VIIRS sensor utilizes a backside-illuminated charge coupled device (CCD) focal plane array (FPA) for sensing of radiances spanning 7 orders of magnitude in one panchromatic (0.5-0.9 μm) reflective solar band (RSB). In order to cover this extremely broad measurement range, the DNB employs four imaging arrays that comprise three gain stages. The low gain stage (LGS) gain values are determined by solar diffuser data. In operations, the medium and high gain stage values are determined by multiplying the LGS gains by the medium gain stage (MGS/LGS) and

Return to Page 1

high gain stage (HGS/LGS) gain ratios, respectively.

Recent work by Shao et al., 2013 demonstrated the use of lunar illumination to perform vicarious radiometric calibration of DNB at night. This is performed by selecting events when Suomi-NPP flies above the vicarious sites such as Dome C in Antarctic and Greenland in the Northern Hemisphere at night and the moon illuminates the site with lunar phase being more than half moon. Dome C is one of the CEOS endorsed vicarious calibration sites with minimal atmospheric effect and has been recommended to be used as a community reference standard for calibration/validation of visible and near-infrared (VNIR) channels (Cao et al., 2010).

Additional event selection criteria such as solar zenith angle >118° and lunar zenith angle < 80° have been applied to ensure that there are no influences of straylight effects and adequate lunar light illuminating on the vicarious sites. The selected cases for analysis occur at perpetual nights for these two regions of interest (ROIs) at high latitude. For Antarctic Dome C, this occurs during May to August each year. For Greenland in the Northern Hemisphere, this occurs during the winter season from November to January. Figure 1 (a,b) shows examples of the DNB observation of Dome C and Greenland, respectively, at night under lunar illumination.

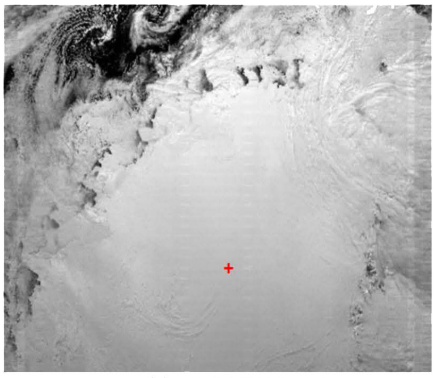

(a) 07/04/2012 15:05

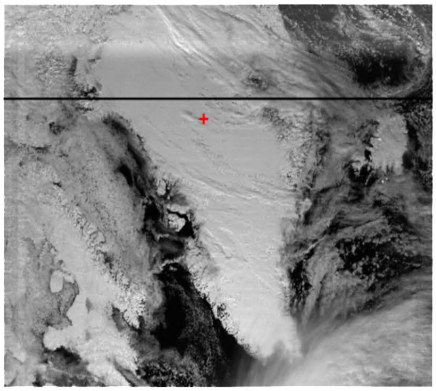

(b) 11/30/2012 06:01

Figure 1 (a, b): DNB observations of Dome C and Greenland, respectively, at night under lunar illumination. Red '+' mark the centers of the vicarious sites used in this study.

The radiance data from DNB observations for the selected events over the year 2012 and 2013 were collected and analyzed to derive the characteristic radiance for the ROI. Lunar spectral irradiance model (Miller and Turner, 2009) (MT2009) as a function of Sun-Earth-Moon distances and lunar phase is used to assist the determination of top-of-atmosphere (TOA) reflectance at the vicarious site. Figure 2 shows the scatter plot of characteristic TOA radiance L_{DNB} of Dome C and Greenland vs. the predicted TOA radiance from the MT2009 model. In predicting the TOA radiance for the ROI, the modeled lunar radiance has been multiplied with the reflectance derived from the Hyperion observations. The coefficient of determination R^2 for modeled radiance vs. observed radiance is 0.989 and root-mean-square-error *rmse* = 0.529. It is understood that the MT2009 the absolute accuracy is of the order of 10-15% so the results here only show the relative agreement between the VIIRS DNB and the model. Nevertheless the consistency is encouraging for using Dome C and Lunar for DNB validation. NIST traceable lunar models will be needed to perform GSICS-quality product validation in the future

Further analysis of the vicariously-derived reflectance from DNB observations shows general agreement with the reflectance derived from Hyperion observations of the vicarious sites. This work demonstrated a scheme of using DNB observation of ground vicarious sites under lunar illumination at night to independently verify the radiometric accuracy of HGS of DNB.

References

Cao, C., Uprety, S., Xiong, J., Wu, A., Jing, P., Smith, D., Chander, G., Fox, N., Ungar, S., 2010, Establishing the Antarctic Dome C Community Reference Standard Site towards consistent Measurements from Earth Observation

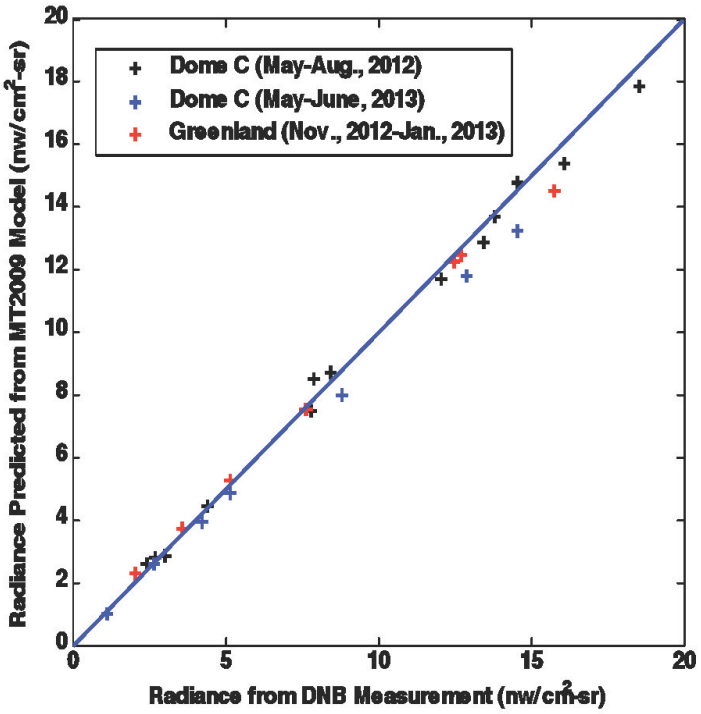

Figure 2: Scatter plot of radiances observed by DNB vs. radiance predicted from Miller and Turner, 2009 (MT2009) model.

Return to Page 1

Satellites. *Canadian Journal of Remote Sensing*, 36, 498-513

Cao, C., DeLuccia, F., Xiong, X., Wolfe, R., Weng, F., 2013, Early on-orbit performance of the Visible Infrared Imaging Radiometer Suite (VIIRS) onboard the Suomi National Polar-orbiting Partnership (S-NPPP)Satellite. *IEEE Trans. Geosci. and Remote Sens.*, 99, 1.

Miller, S.D., and Turner, R.E., 2009, A dynamic lunar spectral irradiance data set for NPOESS/VIIRS Day/Night Band nighttime environmental applications. *IEEE Trans. Geosci. and Remote Sens.*, 47, 2316.

Shao, X., Cao, C., and Uprety, S., 2013, Vicarious calibration of S-NPP/VIIRS day-night band. *SPIE Proceedings Vol. 8866, Earth Observing Systems XVIII*, James J. Butler; Xiaoxiong (Jack) Xiong; Xingfa Gu, Editors, 88661S, DOI: 10.1117/12.2023412.

Rate and comment on this article

Angular Variation of GOES Imager Scan Mirror Visible Reflectivity

by Fangfang Yu, NOAA, Xiangqian Wu, NOAA, Tom Stone, USGS, and Gordana Sindic-Ranic, NOAA

The incidence angle dependent emissivity was observed at the GOES Infrared (IR) channels shortly after the first three axis-stabilized Geostationary satellite began operating in orbit. The variation of the outputs with the east-west (E-W) position of the field of view (FOV) was most apparent when the instruments viewed space. The cause of emissivity variation is believed to be an absorption feature of the silicon-oxide coatings of the scan-mirror. Using space scans as the reference, the IR radiometric calibration accuracy was improved after accounting for the scan-mirror emissivity variation (Weinreb et al. 1998). The angular variation of GOES Imager scan mirror visible reflectivity has been suspected in the GOES visible lunar calibration (Wu et al. 2006) and measured in laboratory (Wu et al. 2011). However, unlike the IR channels, no apparent angular dependent visible space measurements can be observed to use it as the calibration reference to verify the results.

The high relative accuracy of the USGS RObotic Lunar Observatory (ROLO) lunar irradiance model (Kieffer and Stone 2005) makes it possible to use the Moon as the calibration reference to characterize angle dependence of the GOES Imager scan-mirror visible reflectivity. During the GOES-15 post-launch test period, the satellite was rolled northward to trace the Moon as it moved from extreme west to extreme east position across the instrument FOV from ~17:50Z to ~19:20Z on 24 September (DOY267) 2010. During this period of hour and a half, the Imager instrument was pointed to six positions and about one hundred and fifty lunar images were scanned from these six sectors. The Moon's phase angle ranged from 14.4° to 16.5° during this period.

In the lunar calibration, the ratio of measured and modeled lunar irradiance values is often used to describe the sensor performance.

$$R(\mathrm{t}) = \frac{E_{GOES}}{E_{\mathrm{model}}} \qquad (1)$$

where E_{GOES} and E_{model} are the measured and modeled lunar irradiance, respectively.

The GOES lunar irradiance can be calculated as follows:

$$E_{GOES} = \sum_i \left(\frac{\omega_i}{f_i} * (C_i - C_{bk,i}) * S_i\right) \qquad (2)$$

Where ω_i is the solid angle subtended by moon pixel *i* which can be considered as a constant for GOES Imager visible channel, f_i is its oversampling factor, C_i is the pixel (*i*) output signal in count, $C_{bk,i}$ is the background space signal in count, and S_i is the prelaunch calibration coefficient to convert instrument signal output from raw counts to radiance for which the median of the eight visible detectors is used in this study (http://www.star.nesdis.noaa.gov/smcd/spb/fwu/homepage/GOES_Imager_Vis_PreCal.php).

According to the GOES N-P Data Book prepared by ITT et al. (2010), for the visible channels, the combination of scan rate (20 degree/sec) and detector sample rate (21840 samples/sec for visible) is 16 μrad, exceeding the pixel E-W instantaneous geometric field-of-view of 28 μrad. For this reason, the constant oversampling factor of 1.75 was used to calculate the lunar irradiance in the previous lunar calibration study (Wu et al. 2011). The resulted lunar irradiance ratios at different scan angles were reported in Wu et al. (2011), similar to the red dots in Figure 1. Here the mean space count shortly after the most recent space clamp event was used as the background space count ($C_{bk,i}$) in Equation (2).

Figure 1: Scatter-plots of measured to modeled lunar irradiance ratios (red dots) as well as the moon sizes in the images (blue crosses) versus the corresponding scan angles.

The large ratio variation shown Figure 1 could not be explained with the impact of angular dependent reflectivity. The rapid change of the lunar ratios around the sub-satellite point (scan angle=45°) indicated that other factor(s) dominantly contributed to the unexpected variation. A recent thorough investigation of the GOES visible calibration process during this moon-tracing event indicated that the lunar irradiance ratios correlated well with the Moon sizes in the images (Figure 1). This finding strongly suggested that oversampling factor in these images was not a constant value during this period, although the root cause to the varying the oversampling factor is currently not yet known. It was also found that the

Return to Page 1

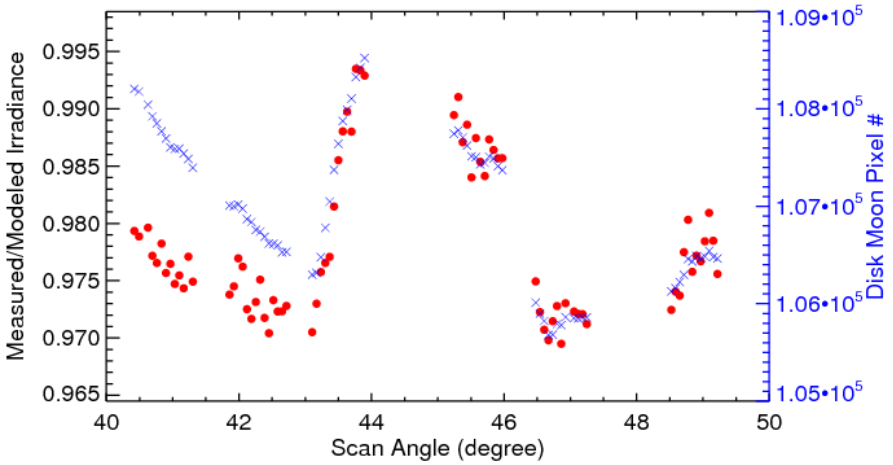

Figure 1: Scatter-plots of measured to modeled lunar irradiance ratios (red dots) as well as the moon sizes in the images (blue crosses) versus the corresponding scan angles.

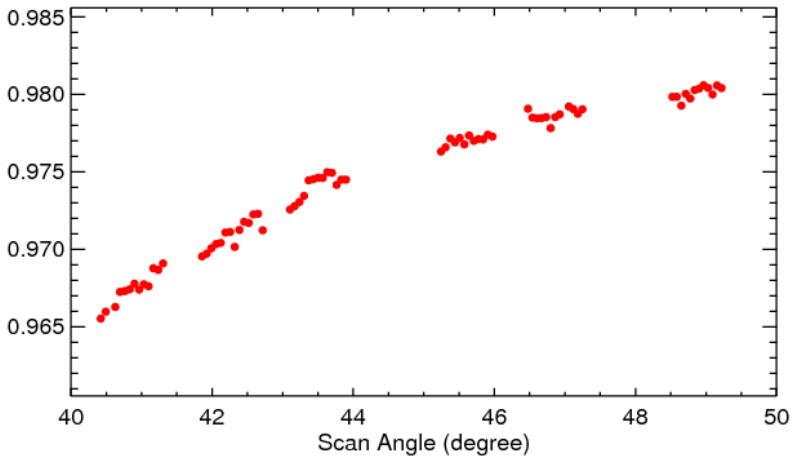

Figure 2: Scatter-plot of measured and modeled lunar irradiance ratios corrected with varying oversampling factors and histogram-derived background space counts versus the scan angles.

background space count, if the pixel is within a certain distance from the Earth or the Moon edge, can be affected with the scattered stray-light that increases as it closes to the Earth or the Moon limb (Yu et al. 2013).

Assuming no significant change in the distance between the moon and satellite during the moon-tracing event, the mean over-sampling factor of a given image is corrected using the normalized moon size as follows:

$$f_i = 1.75 * \frac{A_t}{A_1} \qquad (3)$$

where A_t is the number of moon pixels at time t, A_1 is the number of moon pixels of the first moon image that is used as the reference to normalize the moon size.

To compensate for the possible scattered stray-light effect, the background space count was determined using the second derivative of the histogram of an image that contains both the Moon and space (Wu et al. 2006). Figure 2 displays the new lunar ratios calculated with the varying oversampling factors and the histogram derived background space counts. The large variation in the lunar ratios around the sub-satellite point was completely removed, resulting in a monotonically changing pattern that was similar to those observed at the IR channels and ground measured visible one. The scattering of lunar ratios was also greatly reduced with the histogram-derived background space counts. An about 1.6% reflectance difference was observed between the scan angles at 40° and 50°, which was of the same magnitude but slightly smaller than the laboratory measurement results of 2-3% variation. While further effort should be conducted to investigate the root cause to the varying oversampling factors, a geometric model to calculate the actual moon size at each image will be used to refine the oversampling factor in the future.

Acknowledgement

The authors would like to thank Drs. Kenneth Mitchell and Michael Weinreb for all the valuable discussions about the GVAR data structure and the GOES Imager visible instrument behavior during the radiometric calibration process.

References

ITT Industries, Lockheed Martin and Boeing, 2010, GOES N Series Data Book, Revision C, February 2009, pp 226.

Kieffer, H. and Stone, T, 2005, The spectral irradiance of the Moon, *Astron. J.*, 129, 2887-2901.

Weinreb, M., Jamieson, M., Fulton, N., Chen, Y., Johnson, J., Bremer, J., Smith, C., and Baucon, J., 1998, Operational... calibration of Geostationary Operational Environmental Satellite-8 and -9 imagers and sounders, *Applied Optics*, 36, 6895-6904.

Wu, X., Stone, T., Yu, F., and Han, D., 2006, Vicarious calibration of GOES Imager visible channel using the Moon, *SPIE*, 6296, 62960Z.

Wu, X., Ryan-Howard, D., Stone, T., Sindic-Rancic, G., Yu, F., Weibreb, M., and Grotenhuis, M., 2011, Angular variation of GOES Imager scan mirror reflectance (poster). *Proc. SPIE*, San Diego, CA.

Yu, F., Wu, X., Stone, T., and Sindic-Ranic, G., 2013: Revisit of GOES visible lunar calibration: Error budget and scan-angle dependent reflectance. *CALCON meeting*, Logon, UT.

Rate and comment on this article

Return to Page 1

News in this Quarter

Semi-Annual Meeting of the NOAA/NESDIS Calibration Product Oversight Panel (CalPOP)

by Xiangqian Wu, NOAA

X. Wu chaired this half-day meeting on September 27, 2013. Five of the six panelists and seven invited calibration specialists attended. The panel reviewed the calibration and operation status of instruments on POES (AMSU/MHS, AVHRR, HIRS, and SBUV/2) and GOES (Imager and Sounder) on ten spacecrafts since the last meeting in February 2013. The GSICS Coordination Center (GCC) reported that Larry Flynn and Manik Bali replaced Fuzhong Weng and Fangfang Yu as GCC Director and Deputy Director in April and September, respectively. The GSICS Processing and Research Center at NOAA (GPRC-NOAA) reported progress in GOES Imager visible channel calibration, including the implementation of the DCC- and Moon-based calibration (in coordination with GRWG); the improved calibration based on desert and MODIS (ray-matching); and the advance in integrated calibration. It also updated the operation of GEO-LEO IR inter-calibration.

2013 Field Campaign of Radiometric Calibration for FY Sensors Held at CRCS Dunhuang Site

by Yuan Li, CMA

Under the coordination of the administration office of the Chinese Radiometric Calibration Sites (CRCS), more than 30 persons from 7 Bureaus such as National Satellite Meteorological Center, Gansu Province Meteorology Bureau, National Satellite Ocean Application Service, Anhui Institute of Optics and Fine Mechanics, The Institute of Remote Sensing and Digital Earth, Peking University and Beijing Research Institute of Telemetry have conducted a joint radiometric calibration experiment (CRCS 2013) at Dunhuang site from 11 August to 29 August, 2013 .

The team was divided into four subteams, including atmosphere, surface, infrared, and automatic measurement. We have finished the several vicarious calibration measurements at three phases (12-13, 19-20, and 24-25 August) successfully. 1) The atmosphere subteam measured the aerosol extinction profiles by lidar observation at Dunhuang. Besides the traditional aerosol optic depth, sounding balloons and total

Measurement on the Dunhuang Gobi in 2013

A Note from the Executive Panel Chair

Dr. Mitch Goldberg

I attended the joint AMS and EUMETSAT satellite conference in Vienna in September and was pleased to see the dedicated sessions on instrument calibration and characterization. There were over 30 oral presentations and many more in the poster sessions. Tim Hewison, our GSICS research working group chair, gave a keynote presentation on GSICS activities. The breadth of the presentations continues to emphasize the importance of instrument calibration and intercalibration within the satellite community. GSICS is there to help coordinate activities within an international framework. There has been an increasing call for GSICS to do more in instrument intercalibration beyond the initial focus on geostationary and polar orbiting infrared and visible sensors. As a result the GSICS executive board has agreed to form two new subgroups. These subgroups are for Microwave and Ultraviolet instruments and are being chaired by Dr. Cheng-Zhi Zou and Dr. Larry Flynn (interim), respectively. These join the existing subgroups dedicated to Visible and Infrared that are chaired by Dr. Dave Doelling from NASA and Tim Hewison from EUMETSAT, respectively. Formation of a Modeling sub-group too is envisaged in the near future. This group would focus on inter-comparing satellite measurements with models.

I appreciate the dedication of the entire GSICS team, and a warm welcome to the new chairs of the subgroups.

Return to Page 1

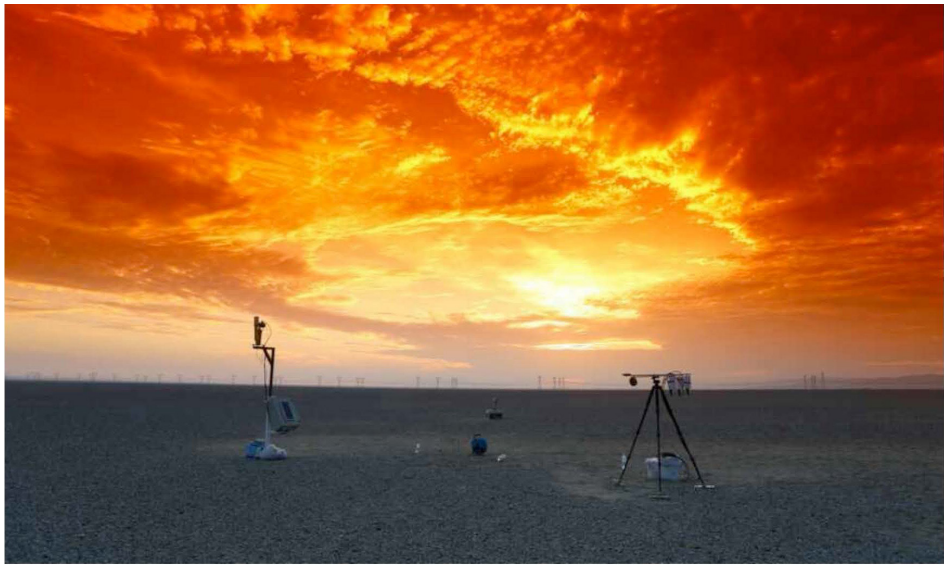

2013 CRCS Dunhuang site under the dawn

and diffuse irradiance, the trace gases contents of OZONE and CO2 were also measured. 2) The surface sub-team used the ASD spectral radiometer to conduct synchronous observation at Dunhuang site. BRDF of Dunhuang site was measured at 9 different positions by portable equipment. 55 surface soil samples were obtained at 11 different positions to analyze the relationship between the distribution of particle size and BRDF. 3) The IR sub-team has performed the continuous measurements of infrared radiance of Dunhuang for several days. 4) The automatic sub-teams used the absolute radiometer to make continuous measurements of spectral and channel radiance of ground surface in several whole days. It's a pre-experiment of completely automatic measurement of radiometric calibration using field measurement.

Improved Accessibility to EUMETSAT GSICS Products

by Tim Hewison, EUMETSAT

Pre-operational GSICS products generated by EUMETSAT are now accessible via our *Product Navigator*: http://navigator.eumetsat.int/. This is a fully searchable index, providing metadata, links to access the data and its documentation.

Furthermore, the GSICS Near-Real-Time Correction for the IR channels of Meteosat10/SEVIRI based on inter-calibration with MetopA/IASI is now being used to generate alternative calibration coefficients. These will soon be inserted into the headers of the operational L1.5 data. (The system is currently running on the validation server). This will allow users to easily calculate the radiances after applying the GSICS Correction, to ensure the calibration is consistent with the GSICS reference, which is currently MetopA/IASI for these IR channels of current sensors. It will also provide a backup in case of problems with the operational on-board calibration system.

FY-3C Satellite was Successfully Launched

by Yuan Li, CMA

At 03:07(UTC) from Taiyuan Satellite Launch Center, September 23, 2013, the carrier rocket CZ-4C lifted off to send FY-3C satellite into predetermined orbit. The launching process is completely successful.

FY-3 is China's second generation of polar-orbiting meteorological satellites, with the goal of observing global atmospheric and geophysical features around the clock, with multiple spectral channels and in three dimensions. The first batch FY-3 includes two testing satellites, FY-3A and FY-3B that were launched May 27th, 2008, and November 5th, 2010, respectively.

The second batch FY-3 is China's second generation of operational polar-orbiting weather satellites. The FY-3C satellite, designed to last 5 years, carries 12 remote sensing instruments, including: Visible Infrared Radiometer, Microwave Scanning Radiometer, Microwave Temperature Sounder, Microwave Humidity Sounder, Microwave Imager, a Medium Resolution Imaging Spectrometer, UV-ozone sounder, Total Ozone UV Detector, Solar Radiation and the Earth Radiation Detector, Space Environmental Monitoring Suits, and GNSS Occultation Detectors. Among them, the Microwave Temperature Sounder and the Microwave Humidity Sounder are upgraded versions. The GNSS Occultation Instrument is a new payload for the global three-dimensional and vertical soundings of the atmosphere.

EUMETSAT Begins Providing Alternative Calibration Coefficients for Meteosat-10/ SEVIRI

by Tim Hewison, EUMETSAT

EUMETSAT is now providing alternative calibration coefficients for Meteosat/SEVIRI based on GSICS Near-Real-Time Corrections, which are derived from comparisons of collocated observations with Metop/IASI. These are provided in the L1.5 image header in the "MPEF Cal Feedback" section. Users can optionally apply these instead of the operation calibration coefficients in the "L1.5 image calibration" section to ensure SEVIRI's calibration is consistent with that of the GSICS reference, and to correct for known radiometric biases in the operational calibration, where these may affect their products. They also provide a backup calibration in case of failure of the on-board system.

Return to Page 1

Announcements

Manik Bali Takes Over as Deputy Director of GSICS Coordination Center

Manik Bali of NOAA's Center for Satellite Applications and Research has been appointed as the new Deputy Director of the GSICS Coordination Center. He is employed through the ESSIC Department of the University of Maryland and replaces Dr. FangFang Yu, who had capably served in the capacity of Deputy Director for the last two years.

Manik has been working in meteorology for the last 15 years. During this time he has worked for C-DAC India, Max Planck Institute for Meteorology Hamburg, Germany, EUMETSAT and European Space Agency and has led national and international projects. He has wide experience in remote sensing; Satellite Calibration, Weather Forecasting and Land – Atmosphere interaction. Mission planning for future ESA missions (Sentinels), Satellite Wind retrieval and Validation of Satellite derived Vegetation Indices are some of the exciting projects he has worked on. Most recently he has been working on the AVHRR re-calibration project at NOAA and developed techniques to use IASI and AIRS radiances to mimic pre-launch environments.

As the Deputy Director of GSICS Coordination Center he will work closely with Larry Flynn (Director, GCC) and members of the GSICS working groups. Enhancing membership of GSICS user communities, evaluation of inter-calibration products and communication among the GSICS members are some of the areas he will focus on.

Manik is an avid cricket, chess, music and beer enthusiast. He works as a freelance journalist and likes to interview scientists and musicians.

Upcoming GSICS-Related Meetings

The next annual meeting of the GSICS Research and Data Management Working Groups will be hosted by EUMETSAT in Darmstadt, Germany on 24-28 March 2014. The invitations will shortly be sent to the official members of the GRWG and GDWG, as well as GSICS Observers and other invited experts. We look forward to seeing you there – so be sure to mark your calendars now!

GSICS Forms UV Subgroup

by Lawrence E. Flynn, NOAA

We are broadening our vision in GSICS to include instruments measuring in the Ultraviolet (UV) portion of the electromagnetic spectrum. There are existing groups and teams, e.g., the CEOS Atmospheric Composition Constellation and the CEOS WGCV Atmospheric Chemistry Subgroup, that are active in research for such instruments but we want to start a focused effort on inter-calibration of spaced-based UV sensors. We will begin by comparing the BUV instruments on polar orbiting platforms. Historically, one of the bases for determining the quality of these instruments' measurements has been comparisons of products to those from limb-based remote sensing. We will need to evolve GSICS to include this approach. There will also be interesting new opportunities for comparisons as BUV instruments are placed on geostationary platforms. We invite member organizations to recommend researchers to participate in this subgroup.

Submitting Articles to GSICS Quarterly Newsletter:

The GSICS Quarterly Press Crew is looking for short articles (~ 700 words with one or two key, simple illustrations), especially related to cal/val capabilities and how they have been used to positively impact weather and climate products. Unsolicited articles are accepted anytime, and will be published in the next available newsletter issue after approval/editing. Please send articles to manik.bali@noaa.gov.

Return to Page 1

GSICS-Related Publications

Chander, G., Angal, A., Taeyoung Choi, and Xiaoxiong Xiong., 2013, Radiometric cross-calibration of EO-1 ALI with L7 ETM+ and Terra MODIS sensors using near-simultaneous desert observations. *IEEE Journal of Selected Topics in Applied Earth Observations and Remote Sensing,* 6, 386–399.

Chen, R., C. Cao, and Menzel, W.P., 2013, Intersatellite calibration of NOAA HIRS CO_2 channels for climate studies. *J. Geophys. Res. Atmos.,* 118, 5190–5203.

Doelling, D., et al., 2013, Desert based Daily Exoatmospheric Radiance Model (DERM) to calibrate collocated geostationary satellites. *Calcon Conf.,* Logan, UT.

Hu, X., et al., 2013, Long-term monitoring and correction of FY-2 infrared channel calibration using AIRS and IASI. *IEEE Transactions On Geoscience AND Remote Sensing*, Vol. 51, 5008–5018.

Liang, X ., Ignatov, A., 2013, AVHRR, MODIS, and VIIRS radiometric stability and consistency in SST bands. *J. Geophys. Res. Oceans,* 118, 3161–3171.

Wang, Z., Xiao, P., Gu, X., Feng, X., Li, X., Gao, H., Li, H., Lin, J., and Zhang, X., 2013, Uncertainty analysis of cross-calibration for HJ-1 CCD camera. *Sci. China Technol. Sci.,* 56, 713–723.

Xu, W., Zheng, X., and Yi, W., 2013, Cross-calibration method based on hyperspectral imager hyperion. *Acta Optica* Sinica, 33, 0528002.

Yu, F., et al., 2013, Inter-calibration of GOES Imager visible channels over the Sonoran Desert. *Calcon Conf.,* Logan, UT.

Special Thanks to Fangfang Yu and George Ohring

The GCC team would like to thank our outgoing Deputy Director Dr. Fangfang Yu. Stationed at NOAA, she joined GSICS activities in 2009 and was appointed as Deputy Director of GCC in Sept. 2011 where she continued till Aug. 2013. She was the main coordinator of GCC activities at NOAA over the past two years and the editor of the Quarterly Newsletter from Oct. 2011 to Jan. 2013. GCC continues to benefit from her experience which she shares from time to time with the incumbent team.

The GCC team would also like to extend special thanks to Dr. George Ohring. George was the Editor of the last two Quarterly Newsletter issues. It was his foresight that resulted in the special issue on Lunar Calibration.

With Help from our Friends:

The GSICS Quarterly Editor would like to thank those individuals who contributed articles and information to this newsletter. The Editor would also like to thank our European Correspondent, Dr. Tim Hewison of EUMETSAT, American Correspondent, Dr. Fangfang Yu of NOAA, GDWG Chair Aleksandar Jelenak, and Asian Correspondent, Dr. Yuan Li of CMA, in helping to secure and edit articles for publication.

GCC team welcomes your feedback and suggestions about the GSICS Newsletter.